THE 24TH CHESAPEAKE SAILING YACHT SYMPOSIUM
ANNAPOLIS, MARYLAND, JUNE 2022

Development of a blockage correction for highly cambered 2D circular arcs

Jean-Baptiste R. G. Souppez, College of Engineering and Physical Science, Aston University, Birmingham, UK (j.souppez@aston.ac.uk).
Ignazio Maria Viola, School of Engineering, Institute for Energy Systems, University of Edinburgh, Edinburgh, UK (i.m.viola@ed.ac.uk).

ABSTRACT

Model-scale testing of yacht sails and wings often suffers from blockage due to the physical constraints of experimental facilities. With blockage, a greater increase in flow speed occurs in the vicinity of the geometry compared to an unblocked flow as a direct consequence of the restricted cross-sectional area. This leads to artificially higher forces, making comparison and validation between tests conducted in different facilities difficult, while also flawing performance prediction if the forces are not suitably corrected. Blockage correction for streamlined bodies and bluff bodies such as flat plates normal to the flow, are well-established. However, it is not the case for lift-generating bluff bodies, or lifting body, experiencing high trailing-edge separation, such as highly cambered plates and downwind yacht sails. This study focusses on the development of a blockage correction for highly cambered plates, specifically circular arcs, comparable to horizontal sections of downwind yacht sails. Measurements are undertaken at positive incidences below deep-stall for Reynolds numbers ranging from 53,530 to 218,000 in a towing tank and a water tunnel to devise a blockage correction. The critical impact of the free surface deformation on wake blockage is evidenced. This allows to set a maximum limit to the amount of blockage a cambered plate can experience before blockage correction is no longer accurate, hence the importance of closed measurement sections to prevent free surface deformation. Furthermore, the experiments revealed that flow behaviours such as the laminar-to-turbulent transition are preserved even with high blockage. The angle of attack at which transition occurs is also preserved in pressurized wind tunnel tests. However, the effect on the forces cannot be fully corrected, and thus further work would be needed to extend the applicability of the proposed blockage correction to such facilities. These findings provide experimental insights into the effect of blockage on highly cambered plates, and it is anticipated they will support future force experiments conducted on high-camber plates and downwind sails in water tunnels.

NOTATION

a	Linear regression coefficient	d	Distance between the two parallel plates for the blockage investigation (m)
a_D	Linear regression coefficient for drag correction		
a_L	Linear regression coefficient for lift correction	f	Chordwise maximum camber location (m)
A_F	Frontal area (m^2)	Re	Reynolds number (chord based)
AR	Aspect ratio (s/c)	s	Span (m)
A_S	Cross-sectional area (m^2)	t	Thickness (m)
b	Linear regression constant	U_∞	Freestream flow velocity ($m.s^{-1}$)
c	Chord length (m)	y_c	Camber (m)
C_D	Drag coefficient		
C_{DB}	Drag coefficient before blockage correction	α	Angle of attack (°)
C_L	Lift coefficient		
C_{LB}	Lift coefficient before blockage correction	PIV	Particle image velocimetry

INTRODUCTION

Model testing undertaken in experimental facilities, such as towing tanks, water or wind tunnels, typically suffers from blockage effects. This is caused by the physical restrictions of the test section compared to the model size. The restricted cross-sectional area leads to an increase in flow speed around the tested geometry compared to an unblocked flow, yielding artificially higher forces. Consequently, blockage correction is a typical part of experimental procedures to correct for wall interference and quantify unconstrained force coefficients. Early work undertaken by Glauert (1933, 1947) proposed a correction for streamlined bodies. Further guidance on wind tunnel experiments and blockage corrections were introduced by Pankhurst & Holder (1952) and later Pope & Harper (1966), more recently updated by Barlow *et al.* (1999). However, these classical wind tunnel blockage corrections remain primarily focused on streamlined bodies.

Bluff bodies have been investigated in the literature, in the form of flat plates normal to the flow. The pioneering work of Allen & Vincenti (1944) provided an early blockage correction, however shown to be only valid for low blockage by Dalton (1971). Maskell (1963, 1965) proposed a more relevant blockage correction, applicable to high blockage. The assumptions underpinning Maskell's work were first improved on by Cowdrey (1968), then Toebes (1971) and later Alexander & Holownia (1978), before a revised blockage correction was proposed by Hackett & Cooper (2001) following extensive testing. Flat plates at 90 degrees to the onset flow remain the major focus of the literature on blockage correction for bluff bodies. This is evidenced the in meta-analysis of Shademan & Naghib-Lahouti (2020), tackling both experimental and numerical studies. Because the research is on stalled wings, the blockage corrections remain limited to the drag only.

Blockage correction for lifting bodies experiencing significant trailing-edge separation therefore remain to be characterized. Examples of such wings are downwind yacht sails, or spinnakers. They operate near stall and feature significant trailing-edge separation (Lasher, 2001; Lasher *et al.*, 2005; Viola & Flay, 2012; Souppez *et al.*, 2019, Souppez *et al.*, 2022). As a result, typical wind tunnel blockage corrections such as that of Pope & Harper (1966) do not prove suitable. Indeed, Arredondo-Galeana (2019) showed the limitation of standard corrections when applied to downwind yacht sails. An investigation into the blockage of lifting bodies is therefore desirable.

Aerodynamic studies have historically been conducted in open, low-speed wind tunnels. Therefore, guidance on the maximum solid blockage recommended for such facilities has been provided. Pope and Harper (1966) originally recommended 10%, which was then revised to 7.5% by Barlow *et al.* (1999). More recently, a value of 5% has been suggested as a maximum to avoid wall interference (Prasanth *et al.*, 2006; Malizia & Blocken, 2020). However, with the advent of flow visualization techniques, such as particle image velocimetry (PIV), that are more easily performed in water, aerodynamic tests are now also undertaken in water tunnels. In the case of downwind sails, this has been the primary means of experimental testing in recent years (Bot *et al.*, 2016; Arredondo-Galeana & Viola, 2017; Souppez *et al.*, 2019; Bot, 2020; Souppez *et al.*, 2021). Water tunnel experiments are undertaken at similar Reynolds numbers (Re), and thus low-speed wind tunnel recommendations regarding blockage are accepted as suitable, but without specific evidence of their application to tests in water. In the case of PIV, larger geometries are desirable to achieve a higher spatial resolution. Hence higher blockage ratios are necessary, and thus an upper limit should be stipulated. There is also a distinction made between open and closed wind tunnel sections, the latter warranting alternative corrections (Malizia & Blocken, 2020). The distinction between open and closed water tunnel sections remains uncharacterized, particularly as the former involves a free surface. Moreover, it is unclear whether blockage does affect flow structures. For instance, on circular cylinders, Xu *et al.* (2003) suggested changes in the downstream flow structures, whereas Wang *et al.* (2021) concluded that the wake was unaffected.

In this paper, a 2D highly cambered circular arc with a sharp leading edge will be studied. This geometry is a paradigm of cambered thin wings, and is representative of the midspan section of a spinnaker. The aim is to quantify the effect of blockage, and devise a blockage correction that would allow comparison of experimental data between two different experimental facilities. Furthermore, the impact of free surface deformation on force measurement will be addressed, together with recommendations for suitable blockage ratios for the experimental testing of cambered plates. The effect of blockage on flow structures, such as the laminar-to-turbulent transition, will also be investigated. It is anticipated these findings will provide insights into the effect of blockage on 2D cambered plates, and help refine future experiments conducted in water tunnels.

The paper is organised as follows. First, the methodology introduces the geometry, the experimental facilities, and the setup for the blockage investigation. Then, the results cover the validation of the force measurements against published data, before tackling the effect of blockage and the resulting correction. Ultimately, the conclusions draw the main findings from this study and its applications, as well as opportunities for future work.

METHODOLOGY

Geometry

A highly cambered, thin circular arc with a sharp leading edge was adopted as simplified 2D geometry for the study of downwind yacht sails. This was originally introduced by Collie (2006), with further investigation into force measurements by Velychoko (2014), and flow visualisation by Bot (2020) and Souppez *et al.* (2021). More recently, the geometry has also been of interest in the context of wind-assisted ship propulsion (Muggiasca *et al.*, 2021, Souppez & Viola, 2021; Khan *et al.*,

2021), particularly for DynaRigs (Bordogna, 2020; Reche-Vilanova *et al.*, 2021).

Three arcs were employed in this study, with chords lengths of 100 mm, 150 mm, and 200 mm, the geometric characteristics of which are detailed in Table 1 and depicted in Figure 1. The camber-to-chord ratio, y_c/c = 0.2232, is identical that tested by Velychko (2014) and Bot (2020). The thickness-to-chard ratio, t/c, is smaller than half of that in previous studies by Velychko (2014), Flay et al. (2017) and Bot (2020), where t/c was between 0.0357 and 0.0400. The surface of the arcs were sanded down to a smooth finish using 2500 grit wet and dry sandpaper, ensuring a hydrodynamically smooth surface (ITTC, 2017).

The multiple chord lengths were necessary to cover a wider range of the Reynolds number (53,530 < Re < 218,000) within the given flow speeds that could be achieved in the towing tank and water tunnel. This also contributed to maintain the forces generated within the operating range of the load cells. Experiments were undertaken at positive angles of attack (α) below deep stall (5° < α < 25°), in 1° increments with an accuracy of 0.025° in both the towing tank and water tunnel.

Table 1 - Geometric definition of the tree circular arcs employed.

Circular Arc	Small Arc	Medium Arc	Large Arc
Chord, c (mm)	100	150	200
Span, s (mm)	370	370	370
Camber-to-chord ratio, y_c/c	0.2232	0.2232	0.2232
Chordwise draft to chord ratio, f/c (%)	0.50	0.50	0.50
Thickness-to-chord ratio, t/c (%)	0.0180	0.0120	0.0090

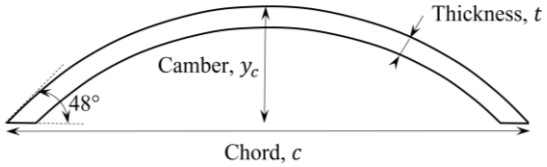

Figure 1 - Experimental geometry.

Towing Tank Testing

Force measurements were realised in the towing tank at Solent University, having a length of 60 m, width of 3.7 m, depth of 1.8 m (Dewavrin & Souppez, 2018). The small (c = 100 mm) arc was tested at Re = 53,530 (as in Velychko, 2014) and Re = 68,200 (as in Bot, 2020); the large (c = 200 mm) arc at Re = 218,000 (as in Bot, 2020); and the medium (c = 150 mm) arc at Re = 150,000. The latter value was arbitrarily chosen to provide intermediate data.

Each arc was fitted between 340 mm long by 340 mm wide end plates to model an infinite aspect ratio. The experimental rig was fitted to a single-post dynamometer equipped with potentiometers having an accuracy of ±0.001 N, and placed in the centre between tank's the side walls. The spanwise axis of the arc was vertical, and the top end-plate 100 mm below the free surface (see Figure 2).

The lift and drag were recorded, once the desired speed was reached, at 1000 Hz for a minimum of six seconds, restricted by the run length. The data acquisition was automatically triggered after the desired test speed was reached. The forces created by the test rig, including end plates, were first measured without the test geometry at the various test speeds. These were later subtracted from the time averaged total force measurement to yield the lift and drag created by the circular arc. This introduces an error because of the interaction between the support structures and the geometry. However, it is assumed that the interaction is negligible, and that the forces can be added linearly. The same approach was applied in the water tunnel. Lift and drag coefficients were computed as

$$C_L = \frac{L}{\frac{1}{2}\rho c s U_\infty^2}, \tag{1}$$

$$C_D = \frac{D}{\frac{1}{2}\rho c s U_\infty^2}, \tag{2}$$

where the density of the water ρ = 998.33 kg.m^{-3} was assumed for fresh water at a measured temperature of 19.4°C, c is the chord, s is the span and U_∞ is the velocity during the force data acquisition.

The amount of blockage was progressively increased in the towing tank by means of adjustable sidewalls (see Figure 2a), the distance between which was reduced down to the blockage experienced in the water tunnel. The side walls were 1200 mm long by 1200 mm wide. A total of four blockages were investigated, namely widths of 3700 mm, 1180 mm, 550 mm and 340 mm, for α = 5°, 10°, 15° and 20°. The 3700 mm width is the full towing tank width, while the 340 mm corresponds to the water tunnel height, therefore yielding an identical blockage. The intermediate values of 1180 mm and 550 mm were driven by the practical ability to fix the side walls to the carriage.

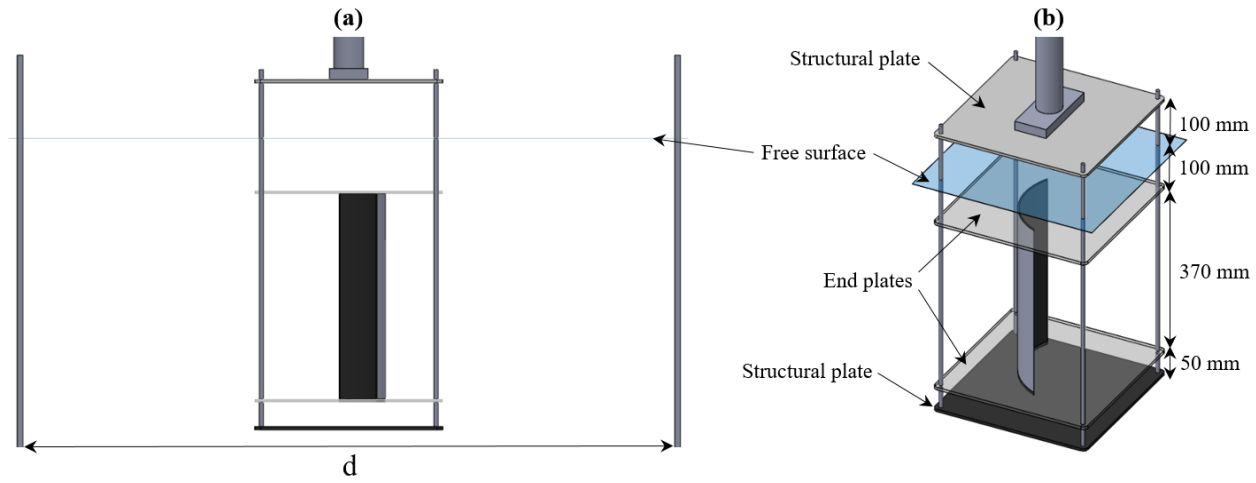

Figure 2 - (a) Side walls setup for the blockage investigation (end elevation), and (b) detailed experimental test rig.

Water Tunnel Testing

Additional force measurements were conducted in the open section water tunnel at the University of Edinburgh. The 8 m long water tunnel features a width of 0.4 m, and a depth of 0.9 m (Arredondo-Galeana & Viola, 2017), with a water level at 0.34 m. The large (c = 200 mm) arc was tested at Re = 68,200, which corresponds to a freestream flow velocity U_∞ = 0.347 m.s^{-1}. This falls within the ideal operating speed ranges for this facility, between 0.25 m.s^{-1} and 0.4 m.s^{-1}, thereby avoiding high turbulence intensity at lower speeds while also preventing significant free surface deformation at higher flow velocities. The arc was vertically centred on the water column, with the suction side towards the free surface. No end plate were fitted as the model spanned across most of the water tunnel's width, with the exception of small gaps either side to avoid contact with side walls and erroneous force measurements. The experimental setup is presented in Figure 3.

The data was sampled using a six-axis force/torque sensor (Nano 17 IP68 from ATI Inc.) with a resolution of 1/160 N, at 100 Hz for 45 seconds. This is substantially longer than the record time in the towing tank, owing to both the limited run length and therefore time in the tank, but also the long period stream fluctuations associated with the recirculation time in the water tunnel. The streamwise turbulence intensity in the water tunnel was measured using laser doppler velocimetry as 3.63% for Re = 68,200. From the work of Arredondo-Galeana (2019), the spanwise flow in this facility is known to be uniform within the central 350 mm of the water tunnel, and unaffected by the bottom boundary layer at the depths where measurements were made. Data was gathered for two distinct conditions: with the free surface allowed to deform due to the pressure changes on the suction side of the geometry, and with a solid top plate restricting any free surface deformation. As such, the latter setup achieves a closed test section, and is most similar to the towing tank experiment.

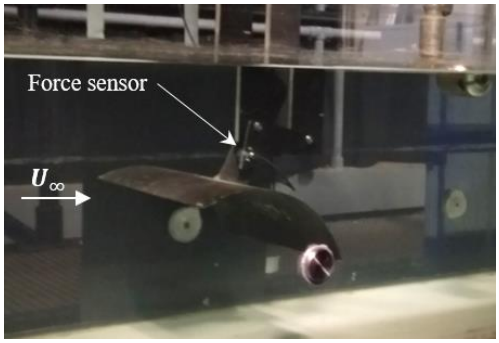

Figure 3 - Water tunnel experimental setup with free surface allowed to deform (no top plate).

RESULTS

Verification of the experimental setup: aspect ratio effect

Towing tank tests at Re = 53,530 are compared with the wind tunnel tests undertaken by Velychko (2014) on an arc with y_c/c = 0.2232 and t/c = 0.0357 at the same Re. The aspect ratio (AR) of the arc in the towing tank is 1.85 and it is equipped with end plates, while the arc in the wind tunnel has AR =10 and it spans across the whole tunnel with the top and bottom walls acting as end plates. The comparison is presented in Figure 4, with error bars corresponding to one standard deviation

for the sampled data. These will be omitted in subsequent figures for clarity. The agreement between the two sets of data suggests that the end plates used in the towing tank are effective in reproducing an arc with an infinite aspect ratio. Furthermore, because the thickness-to-chord ratios of 0.0357 (Velychko, 2014) and 0.0180 provide similar results, we infer that the thickness effect is negligible. Consequently, the results can be generalized to infinitely thin arcs. This is particularly relevant to the model testing of soft downwind sails, having a thickness-to-chord ratio at least one order of magnitude lower than the arcs considered in this study.

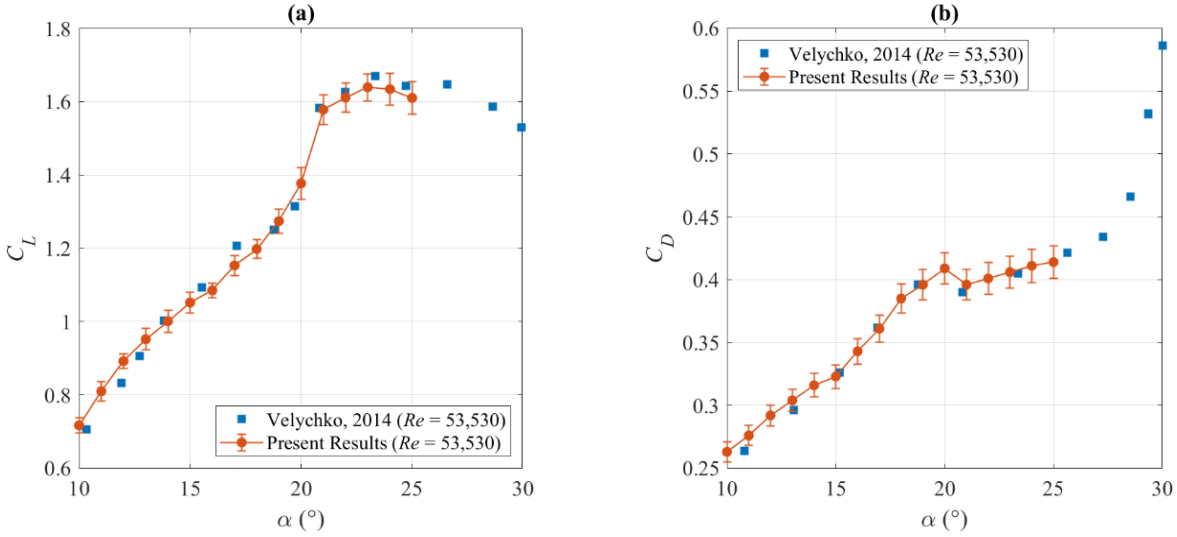

Figure 4 - Aspect ratio effect. Lift (a) and drag (b) coefficients comparison between wind tunnel tests (Velychko, 2014) on an AR = 10 curved plate, and towing tank tests on an AR = 1.85 curved plate at Re = 53,530.

Uncorrected Force Measurements

The results of the towing tank force measurements at all tested Re are depicted in Figure 5, together with the data obtained from the water tunnel at Re = 68,200. Attention is drawn onto the force crisis occurring as a result of the transition from a laminar separation (subcritical regime) to a turbulent one (transcritical regime). This arises from a combination of critical angle of attack and critical Reynolds number (Souppez *et al.*, 2021), and is marked by the sudden discontinuities in forces, measured in steady conditions, for increasing angle of attack. A step-increase in the lift coefficient versus Re curve is present in Figure 5a, with a corresponding reduction in drag coefficient in Figure 5b for the same angle of attack and Reynolds number. This is true for all presented Re, with the exception of Re = 218,000 where this occurs at a lower angle of attack $\alpha < 0°$ (Bot *et al.*, 2016).

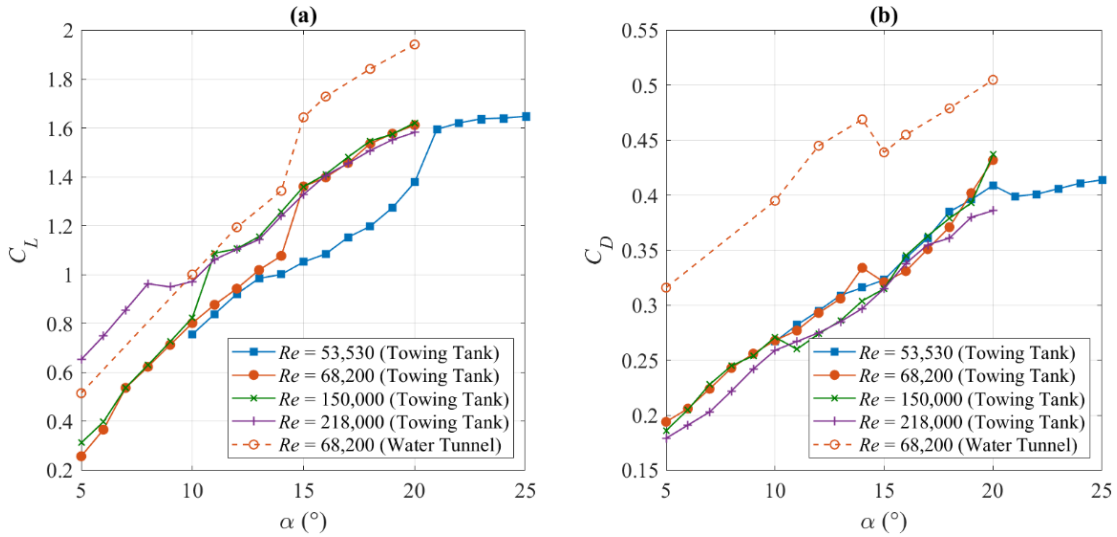

Figure 5 - Force measurements. Lift (a) and drag (b) coefficients recorded in the towing tank and water tunnel.

There is a noticeable offset between the values achieved in the towing tank and those of the water tunnel (with top plate) at Re = 68,200 due to blockage. Here, blockage is defined as the ratio of the frontal area of the geometry, A_F (varying with α), and the area of a virtual cross section $A_S = ds$. For 2D experiments, where the model spans the whole width of the test section, this can also be expressed as the ratio of the frontal height of the model over the height of the test section. Blockage is negligible in the towing tank experiments without sidewalls because the low blockage ratio ($0.30\% < A_F/A_S < 0.47\%$) does not warrant for blockage correction (Barlow *et al.*, 1999). Conversely, blockage is significant in the water tunnel ($14.61\% < A_F/A_S < 24.77\%$). The greater increase in flow speed occurring around the circular arc compared to an unrestricted test section leads to the larger forces.

A key finding is revealed by the two curves at Re = 68,200 in Figure 5 with different blockage values: blockage does not alter the angle of attack at which the laminar-to-turbulent transition occurs in the cases studied. This is a crucial insight because it allows the correct identification of the critical angle of attack regardless of the blockage ratio (at least within the blockage range considered in this work, namely in excess of 20%). It also confirms that the occurrence of turbulent trailing-edge separation is unaffected by blockage. This also justifies using a smooth blockage correction that does not predict non-linear variations associated with changes in the boundary layer state. In fact, in the next section it will be shown that a linear correction allows a good fit of the experimental data.

Blockage Correction

The ratio of the corrected lift and drag coefficients (C_L and C_D) over the recorded values with blockage (C_{LB} and C_{DB}, respectively) decrease with the blockage ratio (A_F/A_S). The results are depicted in Figure 6 for Re = 68,200 (a-b), Re = 150,000 (c-d) and Re = 218,000 (e-f). The presence of two data points for the highest blockage ratio for each angle of attack at Re = 68,200 (Figure 6a and 6b) is because a linear regression was applied to the data gathered from both the towing tank and water tunnel with top plate experiments. This may be seen as a repeat experiment, with the scatter between these points providing an indication of the uncertainty between the two facilities.

The linear regressions of the form $y = ax + b$ yielded a coefficient (a) and a constant (b) for each of the four angles of attack, namely 5°, 10°, 15° and 20°, with the values presented in Table 2. However, as A_F/A_S tends to 0, C_L/C_{LB} and C_D/C_{DB} tend towards 1. The b constant is therefore always 1. For intermediate incidences, the correction equation was achieved using a linear interpolation between the adjacent coefficients. Figure 7a and 7b present the force measurements at Re = 68,200 across the various facilities and setups, prior to blockage correction, while Figure 7c and 7d depict the corrected values. The lift and drag coefficients are obtained using Equations 1 and 2. The relevant values of a given in Table 2, with a_L and a_D respectively used for the lift and drag correction at Re = 68,200, 150,000, and 218,000.

$$C_L = C_{LB}\left(a_L \frac{A_F}{A_S} + 1\right) \tag{1}$$

$$C_D = C_{DB}\left(a_D \frac{A_F}{A_S} + 1\right) \tag{2}$$

Table 2 - Linear regression coefficients.

α	Re = 68,200		Re = 150,000		Re = 218,000	
	a_L	a_D	a_L	a_D	a_L	a_D
5°	-3.3945	-2.6676	-3.7638	-2.6785	-0.6071	-1.4066
10°	-1.0723	-1.7925	-1.2434	-1.4446	-0.7811	-0.8095
15°	-0.7738	-1.3487	-0.7001	-0.3418	-0.6174	-0.4675
20°	-0.6688	-0.6094	-0.3408	-0.2576	-0.3469	-0.2795

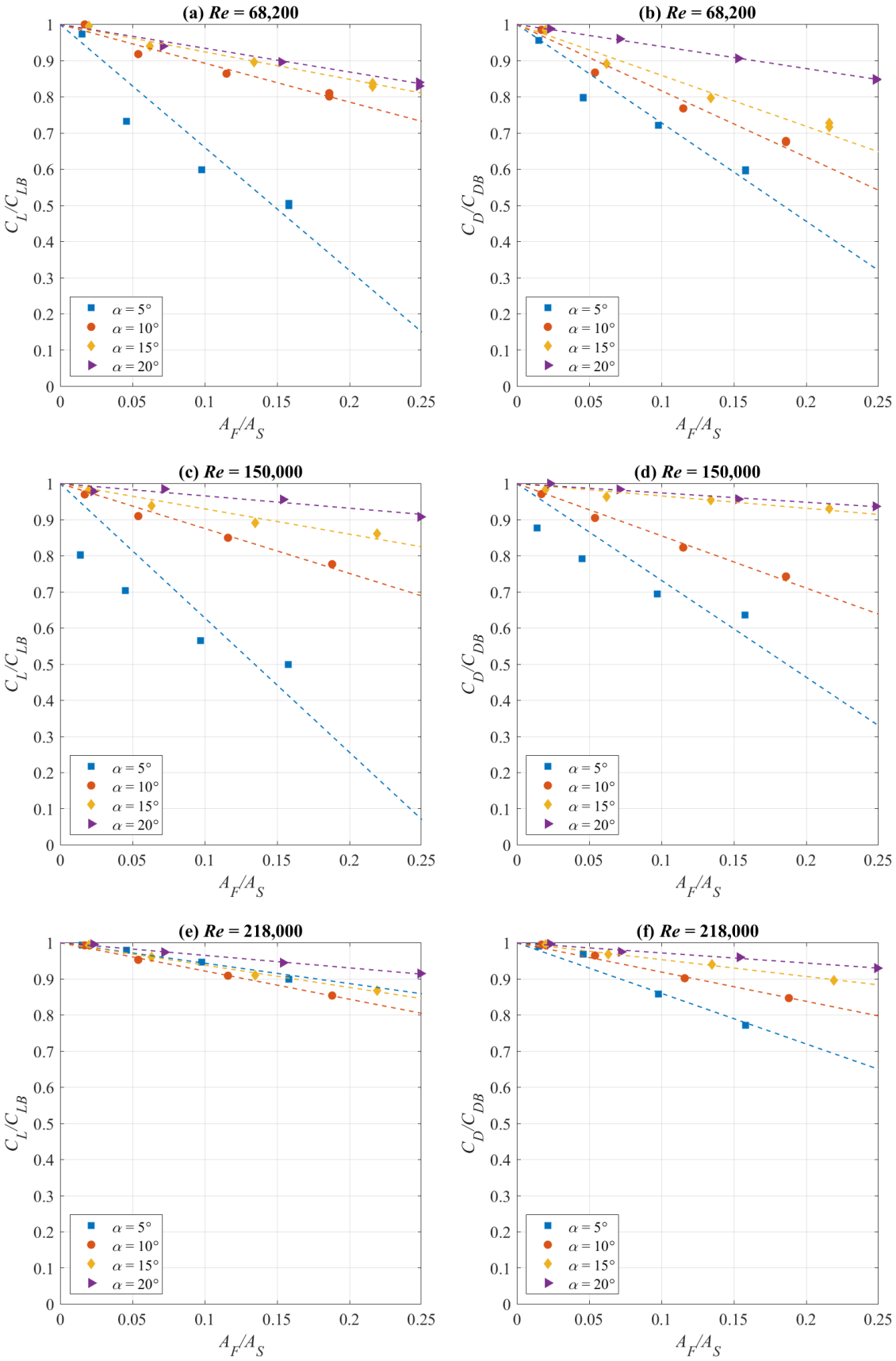

Figure 6 - Ratio of the corrected lift (a) and drag (b) over their measured values versus the blockage ratio for different angles of attack at *Re* = 68,200 (a-b), *Re* = 150,000 (c-d), and *Re* = 218,000 (e-f).

The highest blockage effect is found for $\alpha = 5°$, where the slope of the correction is the highest (Fig. 6). At this incidence, Bot (2020) showed that the stagnation point is on the suction side of the arc, and a large region of recirculating flow occurs on the pressure side of the arc. The blockage seems to affect significantly the forces at this incidence, with less satisfactory linear regressions than for higher incidences. For downwind yacht sail applications, the stagnation is at the leading edge, or on the pressure side of the arc, and $\alpha \geq 11°$ (Souppez *et al.*, 2021). For $\alpha \geq 10°$, the blockage effect is considerably lower and the linear regression is a good approximation of the measured forces.

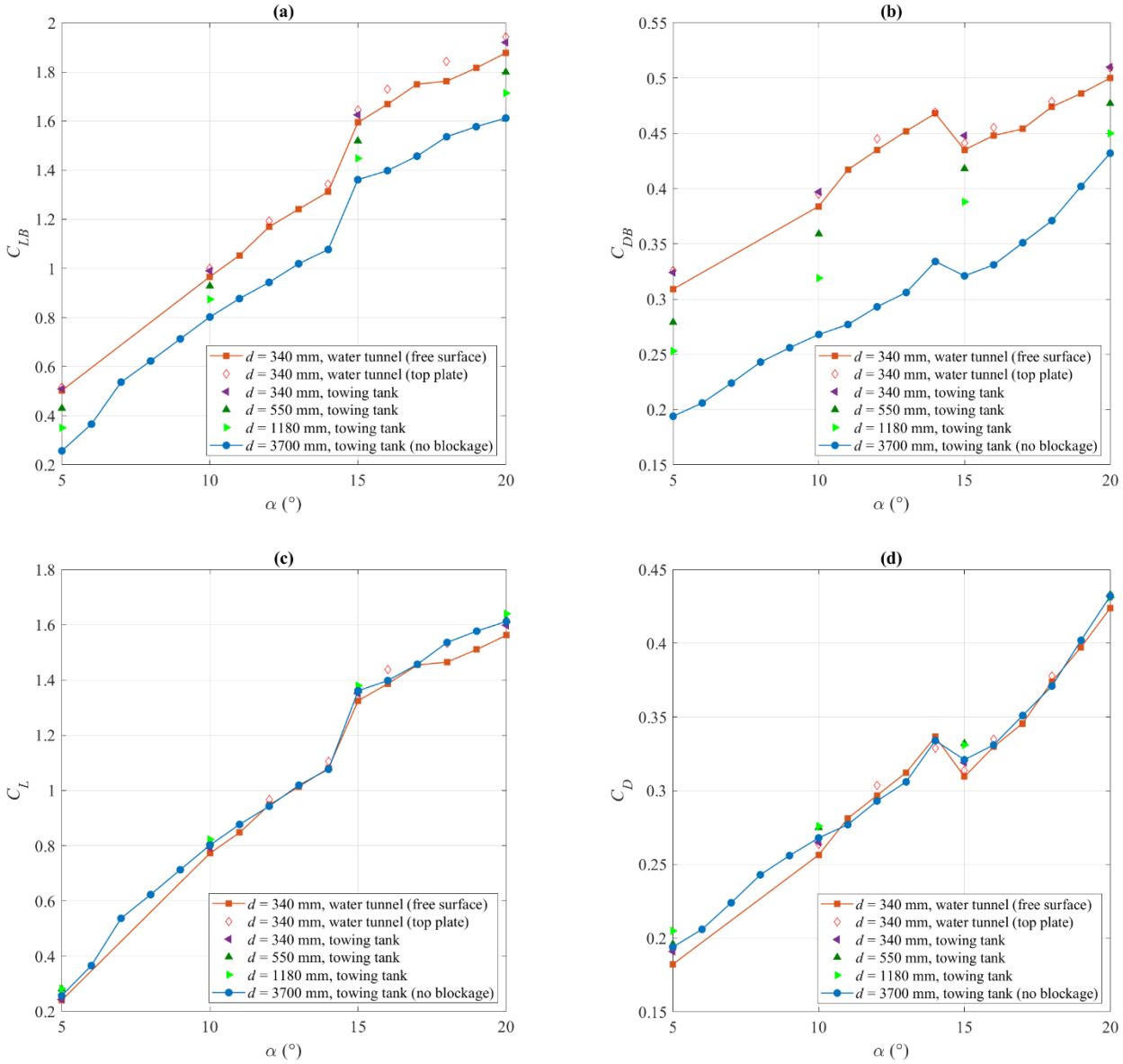

Figure 7 - Measured lift (a) and drag (b) coefficients and corrected lift (c) and drag (d) coefficients at Re = 68,200.

The divergence in the lift coefficient for $\alpha \geq 17°$ in Figure 7c was already present in the measured data (see Figure 7a). It results from free surface deformation at higher incidences, where the wake blockage is greatest, and the solid blockage correction presented in this work less applicable. This can be seen in the discrepancy only occurring for the water tunnel tests where the free surface was allowed to deform, but being absent when a top plate is utilized. This is supported by Arredondo-Galeana (2019), who tested a model-scale spinnaker in the same water tunnel as in this paper. The effect of streamline curvature for highly cambered geometry experiencing high blockage noticeably deformed the free surface, and thus affect the recorded forces. In this instance, the lift coefficient is affected for $A_F/A_S \geq 22.88\%$, and allow to establish an upper limit to the amount of blockage that can be corrected when a free surface is present. It also suggests that a closed section, achieved by means of a top plate for instance, would not suffer from this issue, and thus could cope with higher blockage ratios.

The same methodology was applied to develop a blockage correction at Re = 150,000 and 218,000, with the exception

that tests were only performed in towing tank. Indeed, these Re could not be achieved in the water tunnel because the hydrodynamic moment would have exceeded the maximum range of the load cells. Figure 8 (a-b) presents the measured force coefficients, while the corrected ones are shown in Figure 8 (c-d), for Re = 150,000. The same measured and corrected data is available for Re = 218,000 in Figure 9.

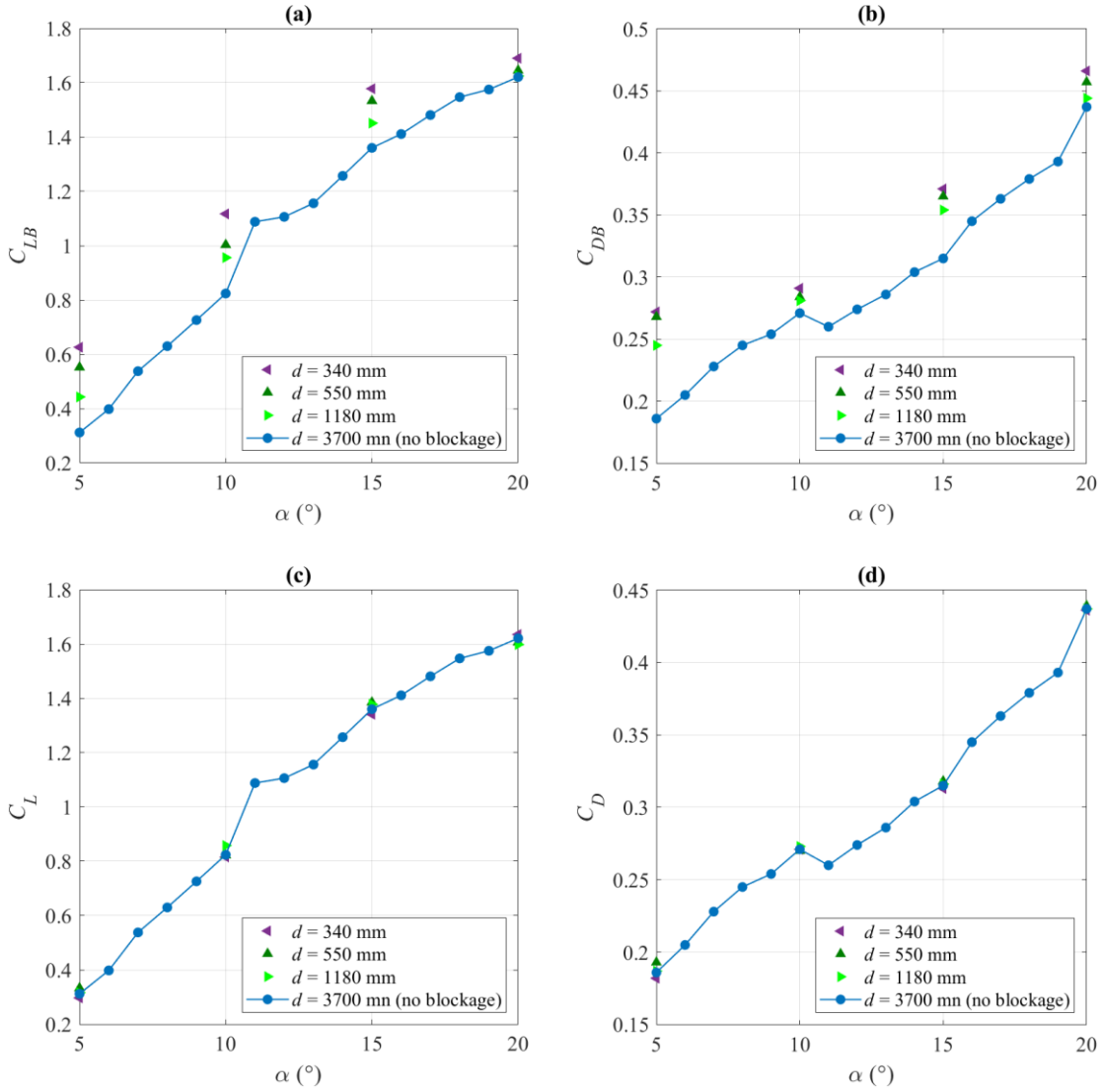

Figure 8 - Measured lift (a) and drag (b) coefficients and corrected lift (c) and drag (d) coefficients at Re = 150,000.

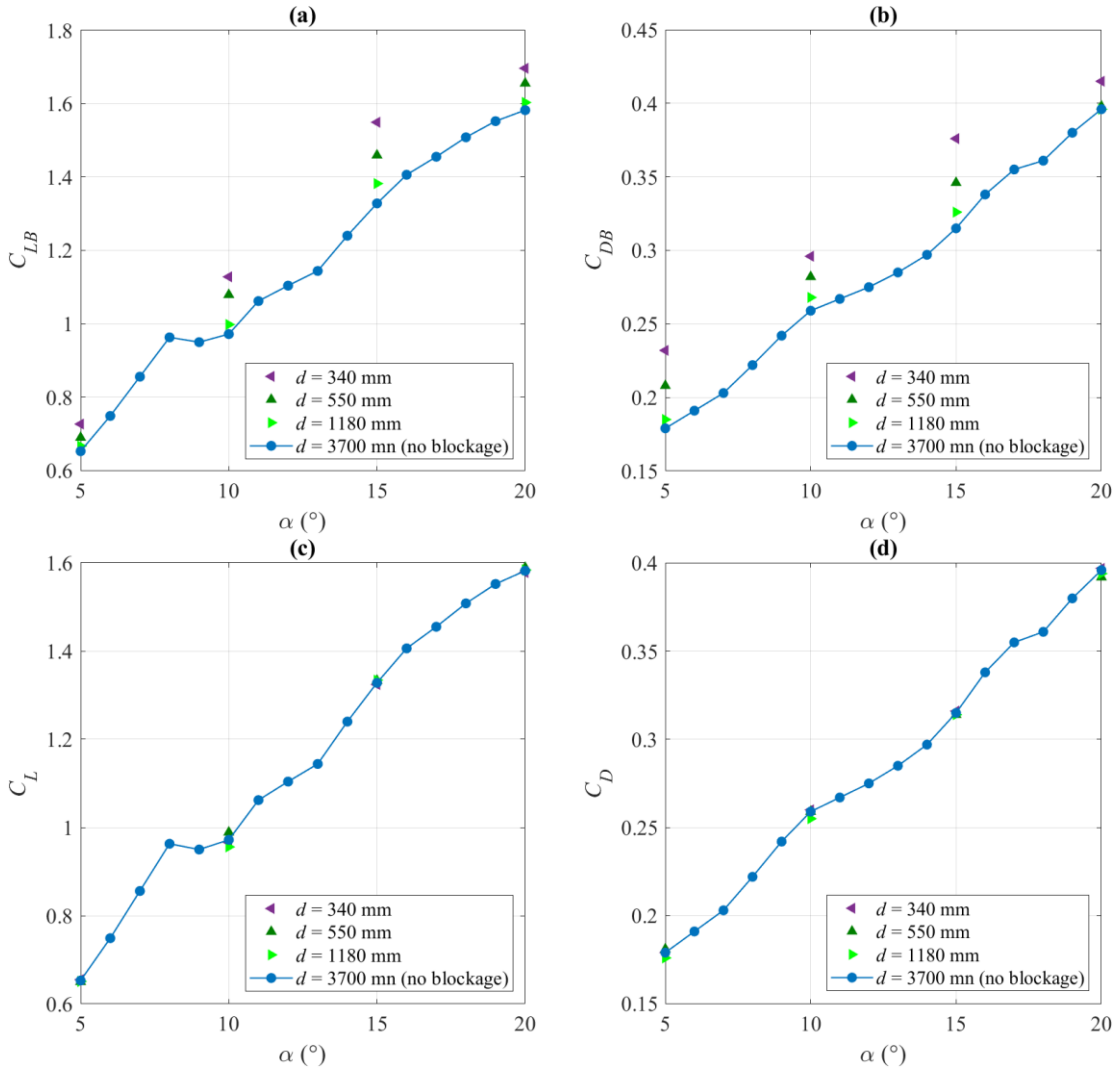

Figure 9 - Measured lift (a) and drag (b) coefficients and corrected lift (c) and drag (d) coefficients at Re = 218,000.

Comparison with pressurized water tunnel

The blockage correction was applied to the results of Bot (2020). An identical circular arc (y_c/c = 22.32%) was also tested at Re = 68,200, but in a pressurized water tunnel, where the test section is located just downstream of a 1/9 contraction. For the lift coefficient shown in Figure 10a, it can be seen that the pressurized water tunnel yielded far greater coefficients. Moreover, the effect of laminar-to-turbulent transition appear to be accentuated, with proportionally greater magnitudes for $\alpha \geq 15°$ (transcritical regime) compared to $\alpha \leq 14°$ (subcritical regime). As a result, the blockage correction devised is not sufficient to accurately correct the lift coefficient, particularly for $\alpha \geq 15°$. On the other hand, the drag coefficients depicted in Figure 10 (b) reveal a fortuitous result. Indeed, the drag correction work perfectly in the laminar region ($\alpha \leq 14°$), but is unsuitable in supercritical condition ($\alpha \geq 15°$). In fact, in this instance, no correction would have been needed in the turbulent flow region. These results are deemed coincidental rather than characteristic of the proposed correction. Indeed, there is a noticeable accentuated effect on the reduction of the drag coefficient in transcritical regime. Further work on applicability to pressurized water tunnel with high contractions should therefore be undertaken.

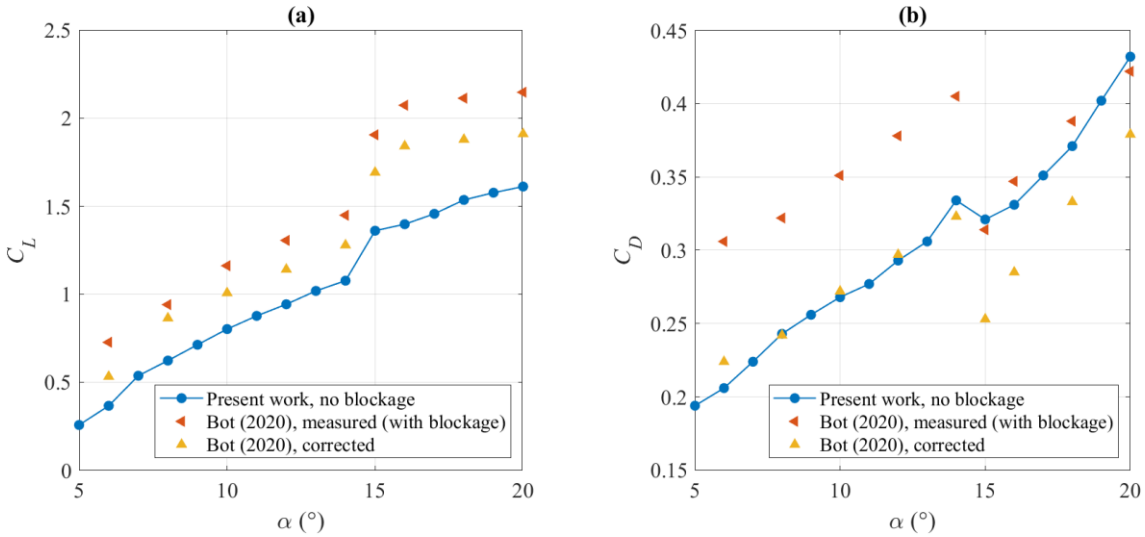

Figure 10 - Application of the blockage correction for (a) the lift coefficients and (b) the drag coefficients of Bot (2020) on an identical circular arc at Re = 68,200.

CONCLUSIONS

Lifting bodies experiencing significant separated flow, such a spinnakers and circular arcs, fall outside of traditional blockage corrections for streamlined bodies or bluff bodies, the latter generally being flat plates normal to the flow. Consequently, force measurements on a 2D circular arc have been undertaken at positive incidences below deep stall, in a transitional Re range. Four blockages were investigated in a towing tank. This allowed to develop an effective blockage correction, applied to measurements gathered in a water tunnel. As a result, force measurements undertaken in different facilities suffering from different blockage ratios can now be compared.

Flow behaviours such as the laminar-to-turbulent transition have been shown to be unaffected by blockage. Indeed, even for blockage ratios in excess of 20%, transition was still identified for the same angle of attack thanks to the characteristic discontinuity in the force coefficients. This result is important to design model-scale sail tests. In fact, full-scale sails always operate at a Re such that the boundary layer is mostly turbulent and laminar trailing-edge separation does not occur. Hence model-scale tests must be performed at higher Reynolds numbers and incidences such that the critical values yielding a turbulent trailing-edge separation are reached. This will yield a flow field representative of that expected at full-scale. The present experimental results reveal that blockage does not affect these critical values.

Furthermore, the effect of the free surface deformation on wake blockage was shown, with a better correction achieved when tests were conducted with a top plate. Achieving a closed test section is therefore recommended. This is particularly critical as blockage could no longer be corrected for $A_F/A_S \geq 22.88\%$ for tests with a free surface. Results suggest higher blockages could still be corrected for in a closed section. This is particularly relevant to PIV experiments undertaken in water tunnels, where larger models are needed to achieve a better spatial resolution, and thus higher blockage ratios are a necessary consequence.

The present work provides experimental insights into the effects of blockage on highly cambered geometries, such as spinnakers, tested in water tunnels. Key flow behaviours such as transition have been shown not to be affected, and the use of a top plate proved to yield more accurate corrections. Extension of the correction to pressurised water tunnels is suggested as future work. These finding will help refine the design of future experiments, while the blockage correction developed will be relevant to separated flow experiments on high-camber wings conducted in water tunnels.

REFERENCES

Alexander, A.J. & Holownia, B.P., *Wind tunnel corrections for savonius rotors*, 2nd International Symposium on Wind Energy Systems, pp. 69-80, 1978.

Allen, H.J., & Vincenti, W.G., *Wall interference in a two-dimensional flow wind tunnel, with consideration for the effect of compressibility*, Technical report No. 782, National Advisory Committee for Aeronautics, 1944.

Arredondo-Galeana, A., *A study of the vortex flow of downwind sails*, PhD Thesis, University of Edinburgh, UK, 2019.

Arredondo-Galeana A., & Viola I.M., *The leading-edge vortex of yacht sails*, Ocean Engineering, 159, pp. 552-562, 2017. https://doi.org/10.1016/j.oceaneng.2018.02.029

Barlow, J.B., Rae, W.H., & Pope, A., *Low-speed wind tunnel testing*, Wiley-Interscience, 3rd edition, 1999.

Bordogna, G., *Aerodynamics of wind-assisted ships*, PhD Thesis, Delft University, 2020.

Bot, P., Rabaud, M., Thomas, G., Lombardi, A., & Lebret, C., *Sharp transition in the lift force of a fluid flowing past nonsymmetrical obstacles: evidence for a lift crisis in the drag crisis regime*, Physical Review Letters, 117, 234501, 2016. https://link.aps.org/doi/10.1103/PhysRevLett.117.234501

Bot, P., *Force variations related to flow patter changes around a high-camber thin wing*, AIAA Journal, American Institute of Aeronautics and Astronautics, pp. 1-7, 2020. https://doi.org/10.2514/1.J058443

Collie, S., *Application of computational fluid dynamics to two-dimensional downwind sail flows*, Auckland: PhD thesis, The University of Auckland, 2006.

Cowdrey, C.F., *Application of Maskell's theory on wind-tunnel blockage to some large-solid models*, Symposium on Wind Effects on Buildings and Structures, Loughborough University, UK, 1968.

Dalton, C., *Allen and Vincenti blockage corrections in a wind tunnel*, AIAA Journal, 9(9), pp. 1864-1865, 1971.

Dewavrin, J.M.M.-A. & Souppez J.-B.R.G., *Experimental Investigation into Modern Hydrofoils-Assisted Monohulls: How Hydrodynamically Efficient are they?*, The Royal Institution of Naval Architects Part B: International Journal of Small Craft Technology, 160(2), pp. 111-120, 2018. 10.3940/rina.ijsct.2018.b2.223

Glauert, H., *Wind tunnel interference on wings, bodies and airscrews*, ARC R&M no 1566, 1933.

Glauert, H. *The elements of aerofoil and airscrew theory*, Cambridge University Press, 2nd Edition, Cambridge, UK, 1947.

Hackett, J.E. & Copper, K.R., *Extensions to Maskell's theory of blockage effects on bluff bodies in a closed wind tunnel*, The Aeronautical Journal, 105, pp. 409-418, 2001. https://doi.org/10.1017/S0001924000012380

International Towing Tank Conference, *ITTC Quality System Manual - Recommended Procedures and Guidelines - Procedure - Ship Models*, 28th International Towing Tank Conference, Wuxi, 2017.

Khan, L., Macklin, J.J.R., Peck, B.C.D., Morton, O., & Souppez, J.-B.R.G., A review of wind-assisted *ship propulsion for sustainable commercial shipping: latest developments and future stakes*, Wind Propulsion 2021, The Royal Institution of Naval Architects, London, UK, 2021.

Lasher, W.C., *Computation of two-dimensional blocked flow normal to a flat plate*, Journal of Wind Engineering and Industrial Aerodynamics, 89, pp. 493-513, 2001.

Lasher, W.C., Sonnenmeier, J.R., Forsman, D.R. & Tomcho, J., *The aerodynamics of symmetric spinnakers*, Journal of Wind Engineering and Industrial Aerodynamics, vol. 93, pp. 311-337, 2005. https://doi.org/10.1016/j.jweia.2005.02.001

Malizia, F., & Blocken, B., *Bicycle aerodynamics: History, state-of-the-art and future perspectives*, Journal of Wind Engineering and Industrial Aerodynamics, 200, 104134, 2020. https://doi.org/10.1016/j.jweia.2020.104134

Maskell, E.C., *A theory of blockage effects on bluff bodies and stalled wings in a closed wind tunnel*, Reports and memorandum 3400, Aeronautic Research Council, 1963.

Maskell, E.C., *A theory of the blockage effects on bluff bodies and stalled wings in a closed wing tunnel*, ARC &M no 3400, 1965.

Muggiasca, S., Bordogna, G., Angelini, G., & Belloli, M., *Experimental study on technologies used for wind-assisted ship propulsion*, IX International Conference of Computational Methods in Marine Engineering (MARINE2021), Edinburgh, 2021.

Reche-Vilanova, M., Hansen, H., & Bingham, H.B., *Performance prediction program for wind-assisted cargo ships*, Journal of Sailing Technology, 6(01), pp. 91-117. https://doi.org/10.5957/jst/2021.6.1.91

Pankhurst, R.C. & Holder, D.W., *Wind tunnel techniques: an account of experimental methods in low- and high-speed wind tunnels*, Pitman, London, UK, 1952.

Pope, A. & Harper, J.J., *Low Speed Wind Tunnel Testing*, John Wiley & Sons New York, 1966.

Prasanth, T.K., Behara, S., Singh, S.P., Kumar, R. & Mittal, S., *Effect of blockage on vortex-induced vibrations at low Reynolds numbers*, Journal of Fluids and Structures, 22(6-7), 99. 865-876, 2006. https://doi.org/10.1016/j.jfluidstructs.2006.04.011.

Shademan, M., & Naghib-Lahouti, A., *Effects of aspect ratio and inclination angle on the aerodynamic load of flat plates*, Advances in Aerodynamics, 2(14), 2020. https://doi.org/10.1186/s42774-020-00038-7

Souppez, J.-B.R.G., Arredondo-Galeana, A. & Viola, I.M., *Recent advances in downwind sail aerodynamics*, 23rd Chesapeake Sailing Yacht Symposium, Annapolis, Maryland, 2019.

Souppez, J.-B.R.G., Arredondo-Galeana, A. & Viola, I.M., *Recent advances in numerical and experimental downwind sail aerodynamics*, Journal of Sailing Technology, 4(01), 45-65, 2019. https://doi.org/10.5957/jst.2019.4.1.45

Souppez, J.-B.R.G., Bot, P. & Viola I.M., *On the effect of the leading-edge separation bubble on the aerodynamics of spinnakers*, 7th High Performance Yacht Design Conference (HPYD7), Auckland, New Zealand, 2021.

Souppez, J.-B.R.G., Bot, P. & Viola I.M., *Turbulent flow around circular arcs*, Physics of Fluids, 34, 015121, 2022. https://doi.org/10.1063/5.0075875

Souppez, J.-B.R.G., & Viola I.M., C*ircular arc aerodynamics and applications to downwind yacht sails and wind assisted ship*, IX International Conference of Computational Methods in Marine Engineering (MARINE2021), Edinburgh, 2021.

Toebes, G.H., *The frequency of oscillatory forces acting on bluff cylinders in constricted passages*, Proceedings of the 14th Congress of the International Association for Hydraulic Research, pp 51-58, 1971.

Velychko, N., *Study of highly cambered aero foil using JR3 sensor*, The University of Auckland, 2014.

Viola, I.M. & Flay, R.G.J., *Sail aerodynamics: on-water pressure measurements on a downwind sail*, Journal of Ship Research, 56(4), pp. 197-206, 2012.

Xu, S.J., Zhou, Y., & So, R.M.C., Reynolds number effects on the flow structure behind two side-by-side cylinders, Physics of Fluids, 15, 1214, 2003. https://doi.org/10.1063/1.1561614

Wang, X., Chen, J., Zhou, B., Li, Y., & Xiang, Z., *Experimental investigation of flow past a confined bluff body: Effects of body shape, blockage ratio and Reynolds number*, Ocean Engineering, 220, 108412, 2021. https://doi.org/10.1016/j.oceaneng.2020.108412

Zilic de Arcos, F., Tampler, G., & Vogel C. R., *Numerical analysis of blockage correction methods for tidal turbines*, Journal of Ocean Engineering and Marine Energy, 6, pp. 183-197, 2020. https://doi.org/10.1007/s40722-020-00168-6